Large-gap two-dimensional topological insulator in oxygen functionalized MXene

Hongming Weng,[1,2,*] Ahmad Ranjbar,[3] Yunye Liang,[4] Zhida Song,[1] Mohammad Khazaei,[5] Seiji Yunoki,[3,6,7] Masao Arai,[5] Yoshiyuki Kawazoe,[4,8] Zhong Fang,[1,2] and Xi Dai[1,2]

[1]*Beijing National Laboratory for Condensed Matter Physics, and Institute of Physics, Chinese Academy of Sciences, Beijing 100190, China*

[2]*Collaborative Innovation Center of Quantum Matter, Beijing, China*

[3]*Computational Materials Science Research Team, RIKEN Advanced Institute for Computational Science, Kobe, Hyogo 650-0047, Japan*

[4]*New Industry Creation Hatchery Center, Tohoku University, Sendai 980-8579, Japan*

[5]*Computational Materials Science Unit, National Institute for Materials Science, 1-1 Namiki, Tsukuba 305-0044, Ibaraki, Japan*

[6]*Computational Condensed Matter Physics Laboratory, RIKEN, Wako, Saitama 351-0198, Japan*

[7]*Computational Quantum Matter Research Team, RIKEN Center for Emergent Matter Science, Wako, Saitama 351-0198, Japan*

[8]*Thermophysics Institute, Siberian Branch, Russian Academy of Sciences, Russia*

(Received 6 July 2015; published 24 August 2015)

Two-dimensional (2D) topological insulators (TIs) have been recognized as a new class of quantum state of matter. They are distinguished from normal 2D insulators with their nontrivial band-structure topology identified by the Z_2 number as protected by time-reversal symmetry (TRS). Two-dimensional TIs have intriguing spin-velocity locked conducting edge states and insulating properties in the bulk. In the edge states, the electrons with opposite spins propagate in opposite directions and the backscattering is fully prohibited when the TRS is conserved. This leads to a quantized dissipationless "two-lane highway" for charge and spin transportation and promises potential applications. Up to now, only very few 2D systems have been discovered to possess this property. The lack of suitable material obstructs further study and application. Here, by using first-principles calculations, we propose that functionalized MXenes with oxygen, M_2CO_2 (M=W, Mo, and Cr), are 2D TIs with the largest gap of 0.194 eV in the W case. They are dynamically stable and natively antioxidant. Most importantly, they are very likely to be easily synthesized by recently developed selective chemical etching of transition-metal carbides (the $M_{n+1}AX_n$ phase). This will pave the way to tremendous applications of 2D TIs, such as "ideal" conducting wire, multifunctional spintronic devices, and the realization of topological superconductivity and Majorana modes for quantum computing.

DOI: 10.1103/PhysRevB.92.075436 PACS number(s): 73.43.Nq, 73.21.−b, 73.61.−r, 71.20.Ps

I. INTRODUCTION

The field of topological insulators (TIs) started from the theoretical proposal of the two-dimensional (2D) TI state in graphene [1–3]. Though the band gap of graphene is too tiny to be observed [4], the conceptual achievement in the band topology has opened the door to the field of topological quantum states (TQSs) [5–7]. The theoretical proposal [8] and experimental verification [9] of 2D TIs in a quantum well of HgTe/CdTe have boosted the quick rising of the field of TIs. The idea of band topology has been extended to three-dimensional (3D) systems [10–12] and other symmetry protected TQSs [13]. Recently, band topology in metals, including the topological Dirac semimetal [14–17], Weyl semimetal [18–23], and node-line semimetal [24–27], has also been intensively studied. Many of the material realizations of these TQSs are first predicted by theoretical calculations and then confirmed by experimental observations [7,28]. The bulk-boundary correspondence of the topological matters is well known now and it is one of the most unique properties of them. For example, 2D TIs are expected to host quantum spin Hall effect (QSHE) with one-dimensional helical edge states, namely, the electrons in such edge states have opposite velocities in opposite spin channels. Thus, backscattering is prohibited as long as the perturbation does not break the time-reversal symmetry (TRS). Such helical edge states are expected to serve as a "two-lane highway" for dissipationless electron transport, which promises great potential application in low-power and multifunctional spintronic devices. Large band-gap 2D TIs are also crucial to realize the long-sought-for topological superconductivity and Majorana modes through proximity effect [6,29]. In this point of view, 2D TIs are more preferred than 3D ones, where the backscattering in the surface states is not fully prohibited.

Compared with the number of well-characterized 3D TI materials, fewer 2D TIs have been experimentally discovered [7,30]. The quantum wells of HgTe/CdTe [9] and InAs/GaSb [31] are among the well-known experimentally confirmed 2D TIs. Both of them require precisely controlled molecular beam epitaxy growth and operate at ultralow temperature. These experimental conditions make further studies difficult and reduce possible applications. There have been many efforts to find "good" 2D TIs, which are expected to have the following advantages: (1) being easy to be prepared, (2) having large bulk band gaps to be operated under room temperature or higher, (3) being chemically stable upon exposure to air, and (4) being composed of cheap and nontoxic elements. The theoretical attempts for predicting good TIs can be roughly classified into two categories: (1) tuning the strength of spin-orbit coupling (SOC), i.e., the band gap, based on a graphenelike honeycomb lattice such as low-buckled silicene [32]; a chemically decorated single layer honeycomb lattice of Sn [33] and Ge [34] or Bi and Sb [35]; and a buckled square lattice BiF [36]; and (2) examining new 2D systems, which might be exfoliated from the 3D layered

*hmweng@iphy.ac.cn

structural materials, such as $ZrTe_5$, $HfTe_5$ [37], and Bi_4Br_4 [38]. Transition-metal dichalcogenide in 1T' [39] and the square-octagon haeckelite [40–42] structure also belong to the latter category. None of the above has been confirmed by experiments yet, though $ZrTe_5$, $HfTe_5$, and Bi_4Br_4 seem to be very promising, since they do exist experimentally and and their single layers are TIs without any additional tuning.

Regarding oxide materials, none of them is known to be a TI in the experiment, though there are several theoretical proposals available in the literature, e.g., 2D TIs in a single layer of iridate Na_2IrO_3 [43], topological Mott insulators [44], Weyl semimetals in pyrochlore $A_2Ir_2O_7$ [18], axion insulators in spinel Osmate [45], and 3D TIs in perovskite of $YBiO_3$ [46] and heavily doped $BaBiO_3$ [47]. It is generally believed that the strong electronegativity of oxygen leads to full ionization of cations and results in ionic bonds with large band gaps, which makes band inversion difficult. However, the noticeable advantages of oxygen compounds, i.e., naturally antioxidant and stable upon exposure to air, have stimulated continuous efforts in searching for new oxide TIs.

In this paper, by using first-principles calculations we demonstrate that functionalized MXenes [48–51] with oxygen, M_2CO_2 with M=W, Mo, and Cr, are 2D TIs. Our phonon calculations indicate that the crystal structures are dynamically stable. The band inversion, which is crucial to the nontrivial band topology, is found to occur among the bonding and antibonding states of M *d* orbitals. The results are robust against the use of different exchange-correlation functional approximations. The bulk band gap of W_2CO_2 is as large as 0.194 eV within the generalized gradient approximation (GGA) and is enhanced to 0.472 eV within the hybrid functional [Heyd-Scuseria-Ernzerhof (HSE06)] [52,53]. Its Z_2 invariant is 1 and has conducting helical edge states. Recently, 2D material MXenes have been successfully obtained by the selective chemical etching of MAX phases—$M_{n+1}AX_n$ (n=1, 2, 3,...), where M, A, and X are a transition metal, an element of group 12–14, and C or N, respectively [54]. The bare surfaces of the MXene sheet are chemically active and are usually terminated by some atoms or chemical groups depending on the synthesis process, which are usually fluorine (F), oxygen (O), or hydroxyl (OH) [55–57]. Therefore, we believe that our proposed M_2CO_2 can be probably realized experimentally in the future and thus will advance the application of TIs greatly.

II. COMPUTATIONAL DETAILS

First-principles calculations were carried out by using the Vienna *ab initio* simulation package (VASP) [58,59]. The exchange-correlation potential was treated within the GGA of Perdew-Burke-Ernzerhof type [60]. SOC was taken into account self-consistently. The cutoff energy for plane-wave expansion is 500 eV and the *k*-point sampling grid in the self-consistent process was $12 \times 12 \times 1$. The crystal structures have been fully relaxed until the residual forces on each atom becomes less than 0.001 eV/Å. A vacuum of 20 Å between layers was considered in order to minimize the interactions between the layer with its periodic images. PHONOPY has been employed to calculate the phonon dispersion [61]. Considering the possible underestimation of the band gap within GGA, the nonlocal HSE06 hybrid functional [52,53] is further supplemented to check the band topology. To explore the edge states, we apply the Green's-function method [7] based on the tight-binding model with the maximally localized Wannier functions (MLWFs) [62,63] of *d* orbitals of M and *p* orbitals of C and O as a basis set. MLWFs are generated by using the software package OpenMX [64,65].

III. RESULTS AND DISCUSSION

The crystal structure of oxygen functionalized MXene is shown in Fig. 1. Bare MXene M_2C is basically a three-layer structure with a trigonal lattice. The C atoms form a layer, which is sandwiched between two M layers. The in-plane sites of M atoms are (1/3, 2/3) and (2/3, 1/3), respectively, of the trigonal lattice of C atoms. The bare surfaces of the MXene sheet are basically terminated by M atoms and they are chemically reactive. Usually, the surfaces are terminated by F, O, or OH depending on the synthesis process. This brings a chance to tune the electronic properties of MXene by appropriate surface functionalization [56,57]. It has previously been shown that MXenes with full surface functionalizations are thermodynamically more favorable than those with partial functionalizations [56], where full surface functionalization requires two chemical groups per cell. As shown in Fig. 1, the oxygen atom might occupy three different sites on the surface, namely, A, B, and T on each surface. Therefore, there are in total six combinations for decoration of two surfaces as listed in Table I. For each case, the crystal structure is

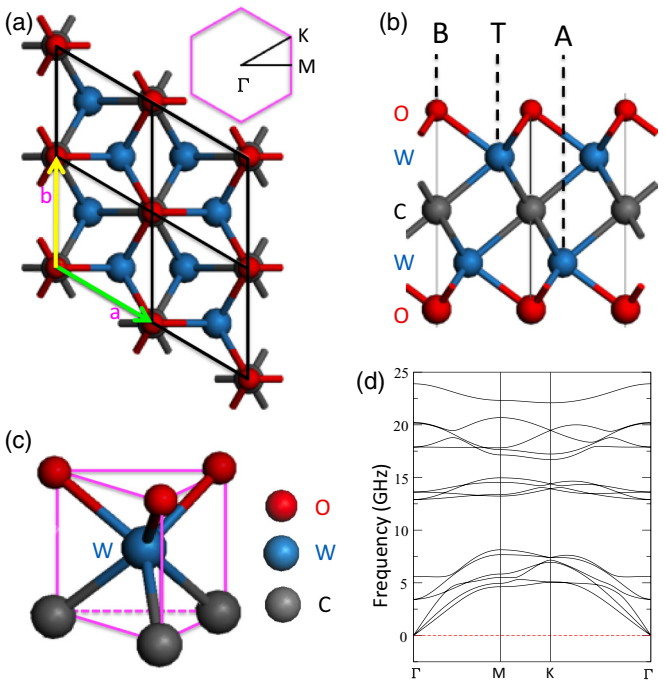

FIG. 1. (Color online) (a) Top view and (b) side view of the optimized crystal structure of W_2CO_2 and its 2D Brillouin zone. There are three possible sites for oxygen decoration on either side of the surface, namely, B (on top of the C site), T (on top of W in the top surface), and A (on top of W in the bottom surface). (c) The triangular prism formed by O and C ions surrounds W. (d) The phonon spectrum for optimized W_2CO_2.

TABLE I. The total energies (in eV per unit cell) for the six possible configurations of W_2CO_2, Mo_2CO_2, and Cr_2CO_2. For each configuration, the structure is fully relaxed. In each unit cell, two oxygen atoms are required for full surface saturations. The symbols T, A, and B indicate three different absorption sites of oxygen atoms as depicted in Fig. 1. All calculations here are performed without spin polarization and within GGA.

Sites of oxygen	W_2CO_2	Mo_2CO_2	Cr_2CO_2
TT	3.162	2.779	1.790
AA	1.189	1.112	0.618
TB	1.828	1.782	1.370
TA	2.024	1.733	1.034
BB	0.0	0.0	0.0
BA	0.878	0.698	0.329

fully relaxed, and the results of total-energy calculations are summarized in Table I. It is observed that MXenes with BB-type oxygen functionalization obtain the lowest energy. In this configuration the M atom sits inside of a trigonal prism formed by the surrounding C and O, which is very similar to the Mo atom in the 1H structure of MoS_2. The phonon spectrum of the energetically stable crystal structure is calculated and shown in Fig. 1(d). Obviously, there is no imaginary frequency, which means such structures are also dynamically stable.

The electronic band structure of W_2CO_2 is shown in Fig. 2. It is found that there is a degenerate band touch point on the Fermi level when SOC is not considered. These degenerate states are mostly composed of $d_{x^2-y^2}$ and d_{xy} orbitals of W atoms as shown by the fat-band analysis. If SOC is further considered, it becomes an insulator. Since it has inversion symmetry, the parity configuration of occupied bands at four time-reversal invariant momenta in the 2D Brillouin zone can be easily obtained and the Z_2 invariant is found to be 1. This indicates that W_2CO_2 is a 2D topological insulator with an indirect band gap as large as 0.194 eV, which can be seen from the inset of Fig. 2(c). The topologically protected conducting edge states have Dirac-cone-like dispersion and connect the bulk valence and conduction bands.

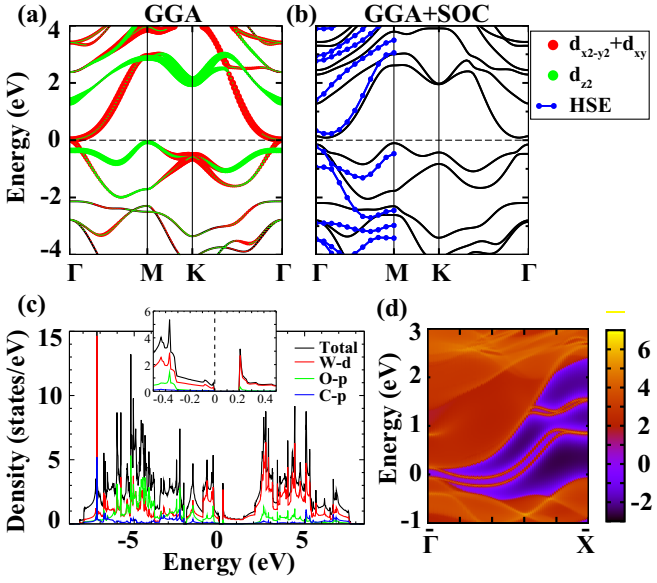

FIG. 2. (Color online) Band structure for W_2CO_2 calculated (a) without and (b) with spin-orbit coupling (SOC). The fat bands are scaled with the projected weight of different atomic orbitals within the eigenstates as shown in (a). The comparison with the bands from hybrid functional (HSE06) calculation including SOC is shown in (b). Total and projected partial densities of states are shown in (c) and the inset has the enlarged plot around the Fermi level (vertical dashed line). The edge states along lattice constant a are shown in (d).

The total and projected partial densities of states, as well as the fat-band plot, clearly show that around Fermi level the W d orbitals are dominant. The p orbitals of C and O are mainly located -2 eV below the Fermi level. The five d orbitals of the W atom are within the triangular prism crystal field of C_{3v} symmetry. The d_{xz} and d_{yz} orbitals are double degenerate and are higher in energy due to the strong hybridization with the p orbitals of C and O. The $d_{x^2-y^2}$ and d_{xy} orbitals are also degenerate and they are around the Fermi level. The d_{z^2} orbital has quite weak hybridization with ligand elements since it points to the center of the ligand triangle. It is also around the Fermi level and slightly lower than $d_{x^2-y^2}+d_{xy}$. Therefore, in order to uncover the low-energy physics of W_2CO_2, we just need to take into account three d orbitals—$d_{x^2-y^2}$, d_{xy}, and d_{z^2}—of the W atoms. It is noticeable that there are two W atoms in one unit cell. As shown in Fig. 3, the above selected d atomic orbitals form bonding and antibonding states. The bonding and antibonding states of d_{z^2} orbitals are even (A_{1g}) and odd (A_{2u}), respectively. Similarly, those from $d_{x^2-y^2}+d_{xy}$ are even (E_g) and odd (E_u) but have double degeneracy. The band inversion happens between the double degenerate E_g and nondegenerate A_{2u} states,which brings the nontrivial topology of bands. When the banding effect is considered from Γ to M, the double degenerate E_g states are split and there is no other band inversion. Further, the SOC introduces the spin degree of freedom and it opens a gap around Fermi level as shown in Fig. 1. Due to the heavy W element, the band gap

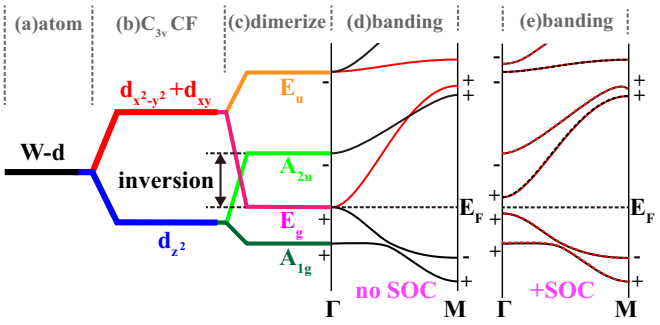

FIG. 3. (Color online) The band inversion mechanism in W_2CO_2. (a) W 5d orbitals are split (b) under the C_{3v} crystal field (CF) with double degenerate $d_{x^2-y^2}+d_{xy}$ and single degenerate d_{z^2} orbitals around Fermi level E_F. (c) The dimerization of two W atoms in each unit cell leads to bonding and antibonding states and band inversion between states with different parities (labeled by + and −). (d) The band dispersion along Γ-M does not induce other band inversion. (e) Including SOC opens the band gap and introduces spin degeneracy in each band, with dashed and solid lines representing opposite spin channels.

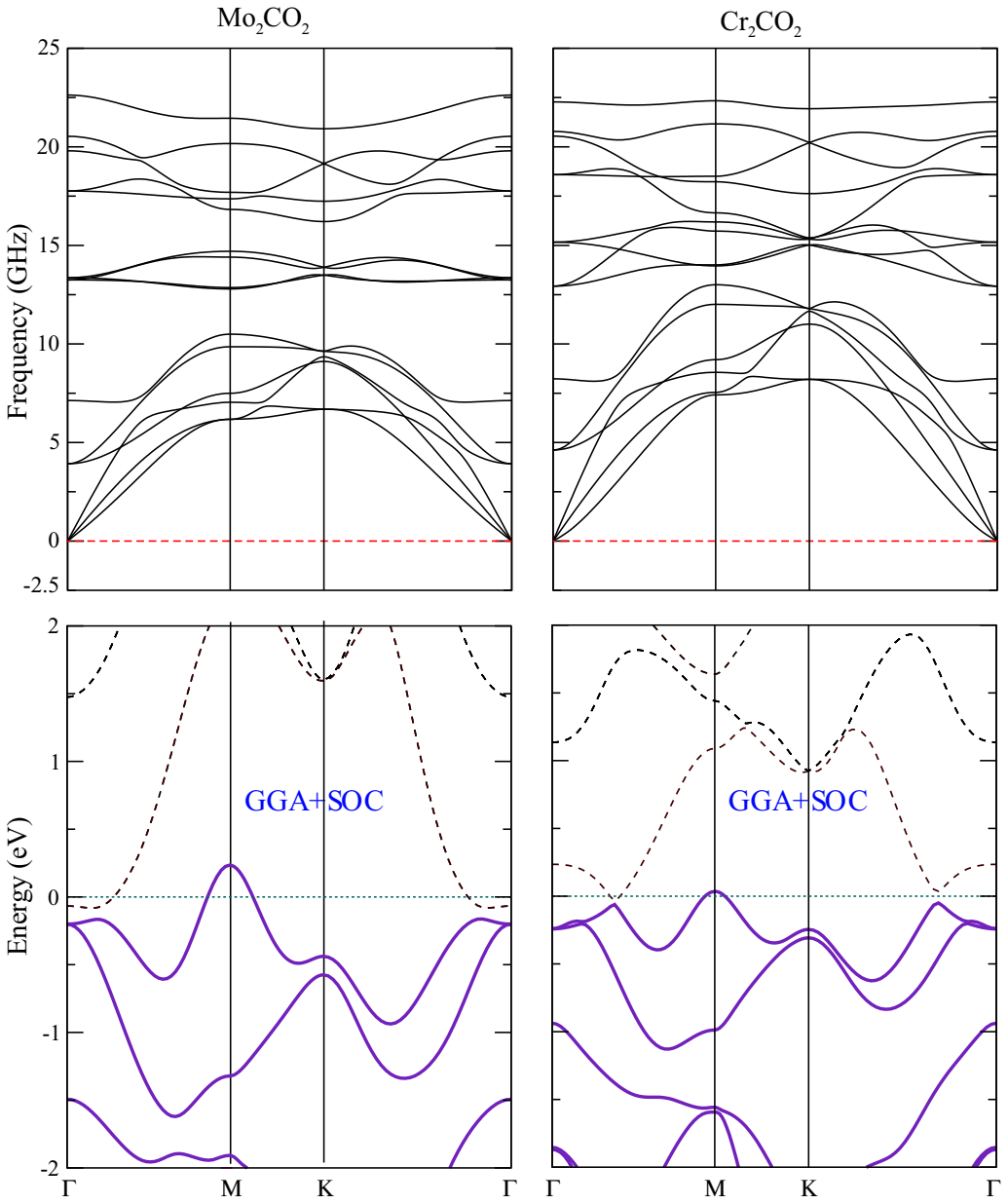

FIG. 4. (Color online) The phonon spectrum (upper panel) and band structure with SOC (lower panel) for optimized stable Mo_2CO_2 (left panel) and Cr_2CO_2 (right panel). The assumed occupied (unoccupied) bands are denoted with solid (dashed) lines.

is found to be as large as 0.194 eV. Considering the possible underestimation of the band gaps within GGA, the hybrid functional (HSE06) calculation is used to check whether the above band inversion around Γ is robust. It is found that the band inversion is kept and the band gap is enhanced to as large as 0.472 eV. Such a large-band-gap 2D TI has an advantage in observing quantum spin Hall effect at room temperature or higher, which is appropriate for device applications.

For Mo_2CO_2 and Cr_2CO_2, both of them have a crystal structure similar to W_2CO_2 and are also dynamically stable as seen from the phonon spectra shown in Fig. 4. Since Mo and Cr have weaker SOC than W, they are expected to have narrower band gaps than W_2CO_2. In fact, both of them show band structures of semimetals by having compensated electron and hole Fermi pockets. However, at each k point, one can still find a well-defined band gap with a curved Fermi level. The assumed occupied bands, as denoted with solid lines in Fig. 4, have the same Z_2 number as W_2CO_2. Therefore, both of them share the same band topology, as well as the underlying physics, with W_2CO_2.

Furthermore, we have investigated the correlation effect in d electrons of transition-metal M. For quite delocalized 5d electrons in W and 4d in Mo, detailed GGA+U (U is the parameter for onsite Coulomb interaction) calculations ($U <$ 4.0 eV) show that the correlation effect is negligible and the ground states of W_2CO_2 and M_2CO_2 are always nonmagnetic. The results discussed above are robust. However, for 3d transition-metal Cr, simple GGA+U ($U >$ 2.0 eV) calculation for BB configuration gives a solution with magnetic properties. The above nonspin polarization calculations for Cr_2CO_2 are

helpful to understanding the band-gap dependence on the atomic number in that column, but not realistic for Cr_2CO_2 itself. However, this gives us the spin degree of freedom in material designs based on MXene, which is very crucial to seeking Chern insulators hosting quantum anomalous Hall effect [66–68]. Detailed studies on the dependence of the U value and magnetic configurations are left for future work.

IV. CONCLUSIONS

Based on first-principles calculations, we have predicted that a family of oxygen functionalized MXenes M_2CO_2 (M=W, Mo, and Cr) is of 2D TIs. The representative W_2CO_2 has robust band inversion, a nontrivial Z_2 invariant, and a large band gap of 0.194 (0.472) eV within GGA (HSE06). It might satisfy all four criteria of a "good" 2D TI: (1) an easier production process by selective chemical etching method; (2) hosting QSHE at ambient condition; (3) high stability and antioxidant upon exposure to air; and (4) low production cost and consisting of environmental friendly elements.

Inspired by these findings, one can naturally think about obtaining more 2D TI candidates in other functionalized MXenes. A large number of MAX (more than 60) [54,69] brings many possibilities of MXene [50] and huge space in finding topologically nontrivial materials. The possible changes would include replacing O^{2-} with F^- or $(OH)^-$ [56,57,70], varying transition-metal M, replacing C with N or B [69], tuning the number of layers n in MXene $M_{n+1}C_n$ [51], etc. Material design or property tailoring with a single change or any combination of the above changes will lead to more and better 2D TIs or Chern insulators.

ACKNOWLEDGMENTS

H.W., Z.F., and X.D. acknowledge support from National Natural Science Foundation of China (Grants No. 11274359 and No. 11422428), the National 973 program of China (Grants No. 2011CBA00108 and No. 2013CB921700), and the "Strategic Priority Research Program (B)" of the Chinese Academy of Sciences (Grant No. XDB07020100). H.W. acknowledges hospitality during his stay in Tohoku University and part of this work has been done there. Y.K. acknowledges the Russian Megagrant project (Grant No. 14.B25.31.0030). Both Y.L. and Y.K. are supported by JST, CREST, "A mathematical challenge to a new phase of material sciences" (2008-2013). Partial calculations were preformed on TianHe-1(A), the National Supercomputer Center in Tianjin, China and the HOKUSAI GreatWave supercomputer system in RIKEN.

[1] C. L. Kane and E. J. Mele, Quantum Spin Hall Effect in Graphene, Phys. Rev. Lett. **95**, 226801 (2005).
[2] C. L. Kane and E. J. Mele, Z_2 Topological Order and the Quantum Spin Hall Effect, Phys. Rev. Lett. **95**, 146802 (2005).
[3] B. A. Bernevig and S.-C. Zhang, Quantum Spin Hall Effect, Phys. Rev. Lett. **96**, 106802 (2006).
[4] Y. Yao, F. Ye, X.-L. Qi, S.-C. Zhang, and Z. Fang, Spin-orbit gap of graphene: First-principles calculations, Phys. Rev. B **75**, 041401 (2007).
[5] M. Z. Hasan and C. L. Kane, *Colloquium*: Topological insulators, Rev. Mod. Phys. **82**, 3045 (2010).
[6] X.-L. Qi and S.-C. Zhang, Topological insulators and superconductors, Rev. Mod. Phys. **83**, 1057 (2011).
[7] H. Weng, X. Dai, and Z. Fang, Exploration and prediction of topological electronic materials based on first-principles calculations, MRS Bulletin **39**, 849 (2014).
[8] B. A. Bernevig, T. L. Hughes, and S.-C. Zhang, Quantum spin Hall effect and topological phase transition in HGTE quantum wells, Science **314**, 1757 (2006).
[9] M. König, S. Wiedmann, C. Brüne, A. Roth, H. Buhmann, L. W. Molenkamp, X.-L. Qi, and S.-C. Zhang, Quantum spin Hall insulator state in HGTE quantum wells, Science **318**, 766 (2007).
[10] L. Fu, C. L. Kane, and E. J. Mele, Topological insulators in three dimensions, Phys. Rev. Lett. **98**, 106803 (2007).
[11] J. E. Moore and L. Balents, Topological invariants of time-reversal-invariant band structures, Phys. Rev. B **75**, 121306 (2007).
[12] R. Roy, Z_2 classification of quantum spin Hall systems: An approach using time-reversal invariance, Phys. Rev. B **79**, 195321 (2009).
[13] C.-K. Chiu, J. C. Y. Teo, A. P. Schnyder, and S. Ryu, Classification of topological quantum matter with symmetries, arXiv:1505.03535.
[14] Z. Wang, Y. Sun, X.-Q. Chen, C. Franchini, G. Xu, H. Weng, X. Dai, and Z. Fang, Dirac semimetal and topological phase transitions in A_3Bi(A=Na, K, Rb), Phys. Rev. B **85**, 195320 (2012).
[15] Z. Wang, H. Weng, Q. Wu, X. Dai, and Z. Fang, Three-dimensional Dirac semimetal and quantum transport in Cd_3As_2, Phys. Rev. B **88**, 125427 (2013).
[16] Z. K. Liu, B. Zhou, Y. Zhang, Z. J. Wang, H. Weng, D. Prabhakaran, S.-K. Mo, Z. X. Shen, Z. Fang, X. Dai, Z. Hussain, and Y. L. Chen, Discovery of a three-dimensional topological Dirac semimetal, Na_3Bi, Science **343**, 864 (2014).
[17] Z. K. Liu, J. Jiang, B. Zhou, Z. J. Wang, Y. Zhang, H. M. Weng, D. Prabhakaran, S. K. Mo, H. Peng, P. Dudin, T. Kim, M. Hoesch, Z. Fang, X. Dai, Z.-X. Shen, D. L. Feng, Z. Hussain, and Y. L. Chen, A stable three-dimensional topological Dirac semimetal Cd_3As_2, Nat. Mater. **13**, 677 (2014).
[18] X. Wan, A. M. Turner, A. Vishwanath, and S. Y. Savrasov, Topological semimetal and fermi-arc surface states in the electronic structure of pyrochlore iridates, Phys. Rev. B **83**, 205101 (2011).
[19] G. Xu, H. Weng, Z. Wang, X. Dai, and Z. Fang, Chern semimetal and the quantized anomalous Hall effect in $HgCr_2Se_4$, Phys. Rev. Lett. **107**, 186806 (2011).
[20] H. Weng, C. Fang, Z. Fang, B. A. Bernevig, and X. Dai, Weyl Semimetal Phase in Noncentrosymmetric Transition-Metal Monophosphides, Phys. Rev. X **5**, 011029 (2015).
[21] B. Q. Lv, H. M. Weng, B. B. Fu, X. P. Wang, H. Miao, J. Ma, P. Richard, X. C. Huang, L. X. Zhao, G. F. Chen, Z. Fang,

X. Dai, T. Qian, and H. Ding, Experimental Discovery Of Weyl Semimetal TaAs, Phys. Rev. X **5**, 031013 (2015).

[22] B. Q. Lv, N. Xu, H. M. Weng, J. Z. Ma, P. Richard, X. C. Huang, L. X. Zhao, G. F. Chen, C. Matt, F. Bisti, V. Strokov, J. Mesot, Z. Fang, X. Dai, T. Qian, M. Shi, and H. Ding, Observation of Weyl nodes in TaAs, Nat. Phys., doi: 10.1038/nphys3426

[23] X. Huang, L. Zhao, Y. Long, P. Wang, D. Chen, Z. Yang, H. Liang, M. Xue, H. Weng, Z. Fang, X. Dai, and G. Chen, Observation of the chiral anomaly induced negative magneto-resistance in 3D Weyl semi-metal TaAs, Phys. Rev. X (to be published), arXiv:1503.01304.

[24] A. A. Burkov, M. D. Hook, and L. Balents, Topological nodal semimetals, Phys. Rev. B **84**, 235126 (2011).

[25] H. Weng, Y. Liang, Q. Xu, R. Yu, Z. Fang, X. Dai, and Y. Kawazoe, Topological node-line semimetal in three-dimensional graphene networks, Phys. Rev. B **92**, 045108 (2015).

[26] R. Yu, H. Weng, Z. Fang, X. Dai, and X. Hu, Topological Node-Line Semimetal and Dirac Semimetal State in Antiperovskite Cu_3 PdN, Phys. Rev. Lett. **115**, 036807 (2015).

[27] Y. Kim, B. J. Wieder, C. L. Kane, and A. M. Rappe, Dirac Line Nodes in Inversion-Symmetric Crystals, Phys. Rev. Lett. **115**, 036806 (2015).

[28] H. Zhang and S.-C. Zhang, Topological insulators from the perspective of first-principles calculations, Phys. Status Solidi **7**, 72 (2013).

[29] L. Fu and C. L. Kane, Superconducting Proximity Effect and Majorana Fermions at the Surface of a Topological Insulator, Phys. Rev. Lett. **100**, 096407 (2008).

[30] Y. Ando, Topological insulator materials, J. Phys. Soc. Jpn. **82**, 102001 (2013).

[31] I. Knez, R.-R. Du, and G. Sullivan, Evidence for Helical Edge Modes in Inverted InAs/GaSb Quantum Wells, Phys. Rev. Lett. **107**, 136603 (2011).

[32] C.-C. Liu, W. Feng, and Y. Yao, Quantum Spin Hall Effect in Silicene and Two-Dimensional Germanium, Phys. Rev. Lett. **107**, 076802 (2011).

[33] Y. Xu, B. Yan, H.-J. Zhang, J. Wang, G. Xu, P. Tang, W. Duan, and S.-C. Zhang, Large-Gap Quantum Spin Hall Insulators in Tin Films, Phys. Rev. Lett. **111**, 136804 (2013).

[34] C. Si, J. Liu, Y. Xu, J. Wu, B.-L. Gu, and W. Duan, Function-alized germanene as a prototype of large-gap two-dimensional topological insulators, Phys. Rev. B **89**, 115429 (2014).

[35] Z. Song, C.-C. Liu, J. Yang, J. Han, M. Ye, B. Fu, Y. Yang, Q. Niu, J. Lu, and Y. Yao, Quantum spin Hall insulators and quantum valley Hall insulators of BiX/SbX (X=H, F, Cl and Br) monolayers with a record bulk band gap, NPG Asia Materials **6**, e147 (2014).

[36] W. Luo and H. Xiang, Room temperature quantum spin Hall insulators with a buckled square lattice, Nano Lett. **15**, 3230 (2015).

[37] H. Weng, X. Dai, and Z. Fang, Transition-Metal Pentatelluride $ZrTe_5$ and $HfTe_5$: A Paradigm For Large-Gap Quantum Spin Hall Insulators, Phys. Rev. X **4**, 011002 (2014).

[38] J.-J. Zhou, W. Feng, C.-C. Liu, S. Guan, and Y. Yao, Large-gap quantum spin Hall insulator in single layer bismuth monobro-mide Bi_4Br_4, Nano Lett. **14**, 4767 (2014).

[39] X. Qian, J. Liu, L. Fu, and J. Li, Quantum spin Hall effect in two-dimensional transition metal dichalcogenides, Science **346**, 1344 (2014).

[40] S. M. Nie, Z. Song, H. Weng, and Z. Fang, Quantum spin Hall effect in two-dimensional transition-metal dichalcogenide haeckelites, Phys. Rev. B **91**, 235434 (2015).

[41] Y. Sun, C. Felser, and B. Yan, Graphene-like Dirac states and quantum spin Hall insulators in the square-octagonal MX_2 (M=Mo, W; X=S, Se, Te) isomers, arXiv:1503.08460.

[42] Y. Ma, L. Kou, Y. Dai, and T. Heine, Quantum spin Hall effect and topological phase transition in two-dimensional square transition metal dichalcogenides, arXiv:1504.00197.

[43] A. Shitade, H. Katsura, J. Kuneš, X.-L. Qi, S.-C. Zhang, and N. Nagaosa, Quantum Spin Hall Effect in a Transition Metal Oxide Na_2IrO_3, Phys. Rev. Lett. **102**, 256403 (2009).

[44] D. Pesin and L. Balents, Mott physics and band topology in materials with strong spin-orbit interaction, Nat. Phys. **6**, 376 (2010).

[45] X. Wan, A. Vishwanath, and S. Y. Savrasov, Computational Design of Axion Insulators Based on 5*d* Spinel Compounds, Phys. Rev. Lett. **108**, 146601 (2012).

[46] H. Jin, S. H. Rhim, and A. J. Freeman, Topological oxide insulator in cubic perovskite structure, Sci. Rep. **3**, 1651 (2013).

[47] B. Yan, M. Jansen, and F. Claudia, A large-energy-gap oxide topological insulator based on the superconductor $BaBiO_3$, Nat. Phys. **9**, 709 (2013).

[48] M. Naguib, M. Kurtoglu, V. Presser, J. Lu, J. Niu, M. Heon, L. Hultman, Y. Gogotsi, and M. W. Barsoum, Two-dimensional nanocrystals produced by exfoliation of Ti_3AlC_2, Adv. Mater. **23**, 4248 (2011).

[49] M. Naguib, O. Mashtalir, J. Carle, V. Presser, J. Lu, L. Hultman, Y. Gogotsi, and M. W. Barsoum, Two-dimensional transition metal carbides, ACS Nano **6**, 1322 (2012).

[50] M. Naguib, V. N. Mochalin, M. W. Barsoum, and Y. Gogotsi, 25th anniversary article: Mxenes: A new family of two-dimensional materials, Adv. Mater. **26**, 992 (2014).

[51] X. Wang, X. Shen, Y. Gao, Z. Wang, R. Yu, and L. Chen, Atomic-scale recognition of surface structure and intercalation mechanism of Ti_3C_2X, J. Amer. Chem. Soc. **137**, 2715 (2015).

[52] J. Heyd, G. E. Scuseria, and M. Ernzerhof, Hybrid functionals based on a screened coulomb potential, J. Chem. Phys. **118**, 8207 (2003).

[53] J. Heyd, G. E. Scuseria, and M. Ernzerhof, Erratum: Hybrid functionals based on a screened Coulomb potential [J. Chem. Phys. **118**, 8207 (2003)], J. Chem. Phys. **124**, 219906(E) (2006).

[54] M. W. Barsoum, The $M_{n+1}AX_n$ phases: A new class of solids: Thermodynamically stable nanolaminates, Prog. Solid State Chem. **28**, 201 (2000).

[55] K. J. Harris, M. Bugnet, M. Naguib, M. W. Barsoum, and G. R. Goward, Direct measurement of surface termination groups and their connectivity in the 2D MXene V_2CT_x using NMR spectroscopy, J. Phys. Chem. C **119**, 13713 (2015).

[56] M. Khazaei, M. Arai, T. Sasaki, C.-Y. Chung, N. S. Venkataramanan, M. Estili, Y. Sakka, and Y. Kawazoe, Novel electronic and magnetic properties of two-dimensional transition metal carbides and nitrides, Adv. Funct. Mater. **23**, 2185 (2013).

[57] M. Khazaei, M. Arai, T. Sasaki, M. Estili, and Y. Sakka, Two-dimensional molybdenum carbides: potential thermoelectric materials of the MXene family, Phys. Chem. Chem. Phys. **16**, 7841 (2014).

[58] G. Kresse and J. Furthmüller, Efficiency of ab-initio total energy calculations for metals and semiconductors using a plane-wave basis set, Comp. Mater. Sci. **6**, 15 (1996).

[59] G. Kresse and J. Furthmüller, Efficient iterative schemes for ab initio total-energy calculations using a plane-wave basis set, Phys. Rev. B **54**, 11169 (1996).

[60] J. Perdew, K. Burke, and M. Ernzerhof, Generalized Gradient Approximation Made Simple, Phys. Rev. Lett. **77**, 3865 (1996).

[61] A. Togo, F. Oba, and I. Tanaka, First-principles calculations of the ferroelastic transition between rutile-type and $CaCl_2$-type SiO_2 at high pressures, Phys. Rev. B **78**, 134106 (2008).

[62] N. Marzari and D. Vanderbilt, Maximally localized generalized Wannier functions for composite energy bands, Phys. Rev. B **56**, 12847 (1997).

[63] I. Souza, N. Marzari, and D. Vanderbilt, Maximally localized Wannier functions for entangled energy bands, Phys. Rev. B **65**, 035109 (2001).

[64] http://www.openmx-square.org.

[65] H. Weng, T. Ozaki, and K. Terakura, Revisiting magnetic coupling in transition-metal-benzene complexes with maximally localized Wannier functions, Phys. Rev. B **79**, 235118 (2009).

[66] R. Yu, W. Zhang, H.-J. Zhang, S.-C. Zhang, X. Dai, and Z. Fang, Quantized anomalous Hall effect in magnetic topological insulators, Science **329**, 61 (2010).

[67] C.-Z. Chang, J. Zhang, X. Feng, J. Shen, Z. Zhang, M. Guo, K. Li, Y. Ou, P. Wei, L.-L. Wang, Z.-Q. Ji, Y. Feng, S. Ji, X. Chen, J. Jia, X. Dai, Z. Fang, S.-C. Zhang, K. He, Y. Wang, L. Lu, X.-C. Ma, and Q.-K. Xue, Experimental observation of the quantum anomalous Hall effect in a magnetic topological insulator, Science **340**, 167 (2013).

[68] H. Weng, R. Yu, X. Hu, X. Dai, and Z. Fang, Quantum anomalous Hall effect and related topological electronic states, Adv. Phys., doi: 10.1080/00018732.2015.1068524.

[69] M. Khazaei, M. Arai, T. Sasaki, M. Estili, and Y. Sakka, Trends in electronic structures and structural properties of max phases: a first-principles study on M_2AlC (M=Sc, Ti, Cr, Zr, Nb, Mo, Hf, or Ta), M_2AlN, and hypothetical M_2AlB phases, J. Phys.: Cond. Matt. **26**, 505503 (2014).

[70] H. Fashandi, V. Ivády, P. Eklund, A. Lloyd Spetz, M. I. Katsnelson, and I. A. Abrikosov, Dirac points with giant spin-orbit splitting in the electronic structure of two-dimensional transition-metal carbides, arXiv:1506.05398.